Comprehensive ctDNA Measurements Improve Prediction of Clinical Outcomes and Enable Dynamic Tracking of Disease Progression in Advanced Pancreatic Cancer

Morten Lapin[1], Karin H. Edland[1], Kjersti Tjensvoll[1], Satu Oltedal[1], Marie Austdal[2], Herish Garresori[1], Yves Rozenholc[3], Bjørnar Gilje[1], and Oddmund Nordgård[1,4]

ABSTRACT

Purpose: Circulating tumor DNA (ctDNA) has emerged as a promising tumor-specific biomarker in pancreatic cancer, but current evidence of the clinical potential of ctDNA is limited. In this study, we used comprehensive detection methodology to explore the utility of longitudinal ctDNA measurements in patients with advanced pancreatic cancer.

Experimental Design: A targeted eight-gene next-generation sequencing panel was used to detect point mutations and copy-number aberrations (CNA) in ctDNA from 324 pre-treatment and longitudinal plasma samples obtained from 56 patients with advanced pancreatic cancer. The benefit of ctDNA measurements to predict clinical outcome and track disease progression was assessed.

Results: We detected ctDNA in 35/56 (63%) patients at baseline and found that it was an independent predictor of shorter progression-free survival (PFS) and overall survival (OS). After initiation of treatment, ctDNA levels decreased significantly before significantly increasing by the time of progression. In some patients, ctDNA persistence was observed after the first chemotherapy cycles, and it was associated with rapid disease progression and shorter OS. Longitudinal monitoring of ctDNA levels in 27 patients for whom multiple samples were available detected progression in 19 (70%) patients. The median lead time of ctDNA measurements on radiologically determined progression/time of death was 19 days ($P = 0.002$), compared with 6 days ($P = 0.007$) using carbohydrate antigen 19–9.

Conclusions: ctDNA is an independent prognostic marker that can be used to detect treatment failure and disease progression in patients with advanced pancreatic cancer.

Introduction

Despite being a relatively uncommon disease, pancreatic cancer is currently the fourth most common cause of cancer-related death in the Western world (1–3). Recent advances in treatment have improved survival for patients with advanced disease (4–6), who make up the majority of patients with pancreatic cancer (3, 7). Nonetheless, the median overall survival (OS) for this patient group is <1 year (4, 5). The tumor marker carbohydrate antigen 19–9 (CA19–9) is currently the only blood-based biomarker in routine clinical use to monitor the treatment response for pancreatic cancer. However, CA19–9 has several drawbacks that limit its clinical value, including poor sensitivity, false positivity in the presence of obstructive jaundice, and false-negative results in Lewis-negative phenotype patients, who are not able to produce CA19–9 (8–10). Consequently, radiological imaging is still required to determine disease progression, with subsequent changes in therapy.

Circulating tumor DNA (ctDNA) has emerged as a promising new tool for predicting clinical outcome and monitoring the treatment response in patients with cancer (11–14). We previously demonstrated that both indirect detection of ctDNA using the total cell-free (cfDNA) concentration and cfDNA fragmentation analyses and direct detection of mutant *KRAS* have prognostic value in patients with advanced pancreatic cancer (15, 16). In a pilot study, we further demonstrated the potential value of using ctDNA to monitor the treatment response in these patients (16). The potential of ctDNA in monitoring patients with pancreatic cancer has also been investigated in several recent studies, demonstrating promising results (17–21). However, the current evidence is based on a limited number of patients, and the majority of prior studies have focused solely on the detection of mutated *KRAS* to detect ctDNA (16–21). In addition, a subset of patients lack *KRAS* mutations (22), and relying on a single marker for detection will reduce the sensitivity of the approach due to the low levels of cfDNA released into the circulation. To improve the detection of ctDNA, we combined the detection of mutations in eight genes frequently mutated in pancreatic cancer using a previously developed hybridization capture next-generation sequencing (NGS) approach, HYTEC-seq (23), with genome-wide copy-number variation analysis. We used the improved detection methodology to explore the application of ctDNA as a prognostic marker, as well as a marker to monitor the treatment response, in a cohort of patients with advanced pancreatic cancer. The results were compared with serological CA19–9 measurements and radiological imaging.

[1]Department of Hematology and Oncology, Stavanger University Hospital, Stavanger, Norway. [2]Department of Research, Stavanger University Hospital, Helse Stavanger HF, Stavanger, Norway. [3]UR 7537 BioSTM, Faculté de Pharmacie de Paris, Université Paris Cité, Paris, France. [4]Department of Chemistry, Bioscience and Environmental Technology, Faculty of Science and Technology, University of Stavanger, Stavanger, Norway.

B. Gilje and O. Nordgård contributed equally as co-senior authors of this article.

Corresponding Author: Morten Lapin, Stavanger University Hospital, 4068 Stavanger, Norway. Phone: 474-723-3151; E-mail: morten.lapin@sus.no

Clin Cancer Res 2023;29:1267–78

doi: 10.1158/1078-0432.CCR-22-3526

Translational Relevance

The only blood-based biomarker in use to monitor the treatment response for pancreatic cancer, carbohydrate antigen 19–9 (CA19–9), has several drawbacks that limit its clinical value. Circulating tumor DNA (ctDNA) has emerged as an alternative blood-based marker, with evidence indicating its prognostic and predictive value across multiple types of cancer. Our study demonstrates that ctDNA can be used as a marker to monitor treatment response and tumor progression in patients with advanced pancreatic cancer. First, detection of ctDNA persistence after initiation of treatment indicates high probability of tumor progression and inferior survival. Second, ctDNA surveillance during follow-up detects disease progression, with a median lead time of 19 days on radiological imaging/time of death compared with 6 days for CA19–9. Future prospective and interventional clinical trials will be required to implement the current findings in clinical practice and improve outcomes for patients with pancreatic cancer.

Materials and Methods

Patients and samples

This study included 56 patients with locally advanced ($n = 8$) or metastatic ($n = 48$) pancreatic cancer admitted to Stavanger University Hospital between September 2012 and October 2020. Patients received first-line treatment with gemcitabine ($n = 7$), gemcitabine plus nab-paclitaxel ($n = 32$), or FOLFIRINOX ($n = 17$). Peripheral venous blood samples (9 mL EDTA tubes) were drawn before initiation of chemotherapy ($n = 56$) and monthly during treatment ($n = 268$). All blood samples were processed within 2 hours of blood draw. The treatment response was defined by a standard disease evaluation of radiological images based on the RECIST 1.1 criteria (24). CA19–9 was determined routinely by an electrochemiluminescence immunoassay. We also analyzed 60 healthy individuals with no prior or current cancer diagnosis as a negative control group. All patients and healthy controls provided written informed consent to participate in the study. The project was conducted in accordance with the Declaration of Helsinki and approved by the Regional Committee for Medical and Health Research Ethics (REK-Vest 2011/475, REK-Vest 2013/1743, REK-Vest 27441).

Isolation of cfDNA from plasma

Blood samples were separated by density centrifugation using Lymphoprep (Axis Shield) density gradient media according to the manufacturer's instructions. We used 4 mL (1–2 mL for the first 8 patients) of plasma (diluted 1:1 in 0.9% NaCl for the density gradient separation protocol) to isolate the total cfDNA using the QIAamp Circulating Nucleic Acid kit (Qiagen) as directed by the manufacturer. The cfDNA was eluted in 40–50 μL of Buffer AVE (Qiagen) and stored at −80°C until further analysis. In each sample, the cfDNA concentration was determined for mononucleosomal and dinucleosomal DNA using the Agilent High-Sensitivity DNA kit on an Agilent 2100 Bioanalyzer.

Library preparation and sequencing

The library preparation for the HYTEC-seq procedure was described in detail in a previous publication (23). Briefly, we constructed sequencing libraries by ligating Y-adapters containing unique molecular identifiers (UMI) to cfDNA fragments using the Kapa HyperPrep Kit (Roche) according to the manufacturer's instructions. The libraries were subjected to target capture using the SureSelect Target Enrichment System for Sequencing on Ion Proton (Agilent Technologies) and a capture panel covering eight genes frequently mutated in pancreatic cancer (*KRAS*, *TP53*, *SMAD4*, *CDKN2A*, *ARID1A*, *TGFBR2*, *RNF43*, and *GNAS*). Four to 16 capture libraries were combined and loaded onto a PI chip for deep sequencing (~2,500 x/ng input) on an Ion Proton instrument (Thermo Fisher Scientific) using the Ion PI Hi-Q Sequencing 200 chemistry (Thermo Fisher Scientific).

Bioinformatic processing of HYTEC-seq data

The HYTEC-seq bioinformatics pipeline was previously described in detail (23). Briefly, signal processing, base calling, quality control, adapter trimming, sample barcode de-multiplexing, and alignment were performed using the Ion Torrent Suite Software Server (version 5.12) and default settings, except for blind calibration for the base calling. On-target reads were extracted from aligned BAM files using samtools (version 1.8; ref. 25). Remaining adapter sequences were removed and the molecular tag sequence extracted with a locally developed Python script called TagXtractor (https://github.com/oddmundn/TagXtractor). Subsequently, reads were re-aligned to the reference genome using BWA-MEM (version 0.7.17; ref. 26), producing aligned and sorted BAM files. Single-strand consensus sequences (SSCS) were generated from the BAM files by a Python script called SSCScreator (version 1.3, https://github.com/oddmundn/SSCScreator), which used both the molecular tag and genome alignment position to combine reads originating from the same original cfDNA molecule. Subsequently, the forward and reverse SSCS files were combined and aligned to the reference genome with BWA-MEM. Aligned SSCS BAM files were subjected to variant calling using a locally developed R script called PlasmaMutationDetector2 (version 1.1.11, https://cran.r-project.org/web/packages/PlasmaMutationDetector2), which we derived from the previously published package PlasmaMutationDetector (27). Sequencing data from healthy control plasma samples were used to build a background error profile, which was applied for error filtering of the patient sample sequencing data. Only variants that were not known SNPs using the ExAC release 1.0 database, were not indels shorter than three bases, and had significantly higher relative allele frequencies in the patient sample compared with the error profile were called. We also required a minimum SSCS coverage of 100 in a variant position, limited strand bias, and the presence of both forward and reverse SSCSs supporting the variant. Indels shorter than three bases were called with VarScan2 in somatic mode using a healthy control as the normal input to filter recurrent sequencing errors (28). A somatic P value of < 0.001 was required for calling candidate indels. Subsequently, each candidate was visually inspected in Integrated Genomics Viewer (version 5.01) to exclude homo-polymer and mapping errors. For follow-up samples, variants detected by PlasmaMutationDetector2 in prior samples from the same patient were called as long as the variant was present in both forward and reverse SSCSs, and as long as the fraction of reads supporting the variant in the sample was higher than the fraction in control samples. Variant annotation was supported by ANNOVAR software (version 2018–04–16).

Copy-number aberration analysis

Copy-number analysis was performed using the Python library CNVkit (version 0.9.5; ref. 29) in Python 3.6.5. CNVkit infers CNAs from targeted capture sequencing data. Sequencing data from our HYTEC-seq pipeline, including both on-target and off-target reads, were used as input. Only one read per SSCS family was required to

build SSCSs to retain off-target data. Bin sizes were set to default (267, minimum size 200) for the on-target region (eight gene panel) and 500,000 for the off-target region to produce bins containing a similar number of reads. The short arms (p) of acrocentric chromosomes 13, 14, 15, 21, 22, and Y were excluded from the analysis because no reads aligned to these positions. In addition, problematic regions of the genome known to cause signal artifacts according to the CNVkit package and ENCODE blacklist (30) were excluded. A reference file was built from 20 healthy controls; read depths were median-centered and bias-corrected (GC-content, sequence repeats, target density) to produce normalized $\log_2$ read-depth values for each bin. To infer copy-number changes, "observed" normalized $\log_2$ read-depth values from patient samples were subtracted from the "expected" values in the reference file and bins segmented using circular binary segmentation with the "drop-low-coverage" option. Samples with high numbers of bins lacking representation (>5%) and samples failing normalization [skewed median $\log_2$ values (>0.05 or ←0.05) without significant copy-number changes] were considered spurious and excluded from the analysis. To use CNA as a surrogate of ctDNA, we computed a global z-score for each patient sample to approximate the general aneuploidy. First, abnormal representation of each chromosome arm was determined by computing the weighted mean $\log_2$ value of each chromosome arm and calculating a z-score using weighted mean $\log_2$ values for the respective chromosome arm in the 20 healthy control samples. The global z-score was then computed in each sample by summing the square z-scores for each chromosome arm.

Digital droplet PCR

To validate variants detected by HYTEC-seq and detect possible clonal hematopoiesis of indeterminate potential (CHIP, chromatin immunoprecipitation) variants, mutation-specific digital droplet PCR (ddPCR) assays were performed on the QX200 Droplet Digital PCR system (Bio-Rad) according to the manufacturer's instructions, using

Table 1. Baseline patient characteristics stratified according to ctDNA status.

Variable	All patients ($n = 56$)	ctDNA positive ($n = 35$)	ctDNA negative ($n = 21$)	*P*
Median age (range)	67 (41–81)	66 (41–81)	67 (46–79)	0.722
Sex (%)				0.025
Female	21 (38)	9 (26)	12 (57)	
Male	35 (62)	26 (74)	9 (43)	
Median cfDNA level (ng/mL plasma; range)	10.3 (1.4–2,263.1)	14.2 (1.5–2,263.1)	3.4 (1.4–12.4)	1.3E−04
Median mode cfDNA fragment size (bp; range)	166 (164–168)	166 (164–167)	167 (165–168)	3.3E−04
Median CA19–9 U/mL (range)	885 (5–102,041)	2,354 (5–102,041)	280 (5–28,936)	0.068
Primary tumor location (%)				0.011
Head	20 (36)	9 (26)	11 (52)	
Body	10 (18)	5 (14)	5 (24)	
Tail	13 (23)	13 (37)	0	
Not applicable or multi-centric	13 (23)	8 (23)	5 (24)	
Clinical T-stage (%)				0.315
T1	1 (2)	0	1 (5)	
T2	16 (28)	11 (31)	5 (24)	
T3	11 (20)	9 (26)	2 (9)	
T4	23 (41)	12 (34)	11 (53)	
TX	5 (9)	3 (9)	2 (9)	
Clinical N-stage (%)				0.389
N0	18 (32)	9 (26)	9 (43)	
N1–2	27 (48)	18 (51)	9 (43)	
NX	11 (20)	8 (23)	3 (14)	
Clinical M-stage (%)				0.042
M0	8 (14)	2 (6)	6 (29)	
M1	48 (86)	33 (94)	15 (71)	
Metastatic location (%)				0.149
Liver	12 (25)	8 (24)	4 (27)	
Lung	2 (4)	0	2 (13)	
Peritoneal carcinomatosis	2 (4)	1 (3)	1 (7)	
Multiple	32 (67)	24 (73)	8 (53)	
ECOG (%)				0.142
0	9 (16)	3 (8)	6 (29)	
1	35 (63)	24 (69)	11 (52)	
2	12 (21)	8 (23)	4 (19)	
First-line treatment (%)				0.321
Gemcitabine	7 (13)	6 (17)	1 (5)	
Gemcitabine + nab-paclitaxel	32 (57)	20 (57)	12 (57)	
FOLFIRINOX	17 (30)	9 (26)	8 (38)	
Prior anticancer surgery (%)				0.066
Yes	47 (84)	3 (9)	6 (29)	
No	9 (16)	32 (91)	15 (71)	

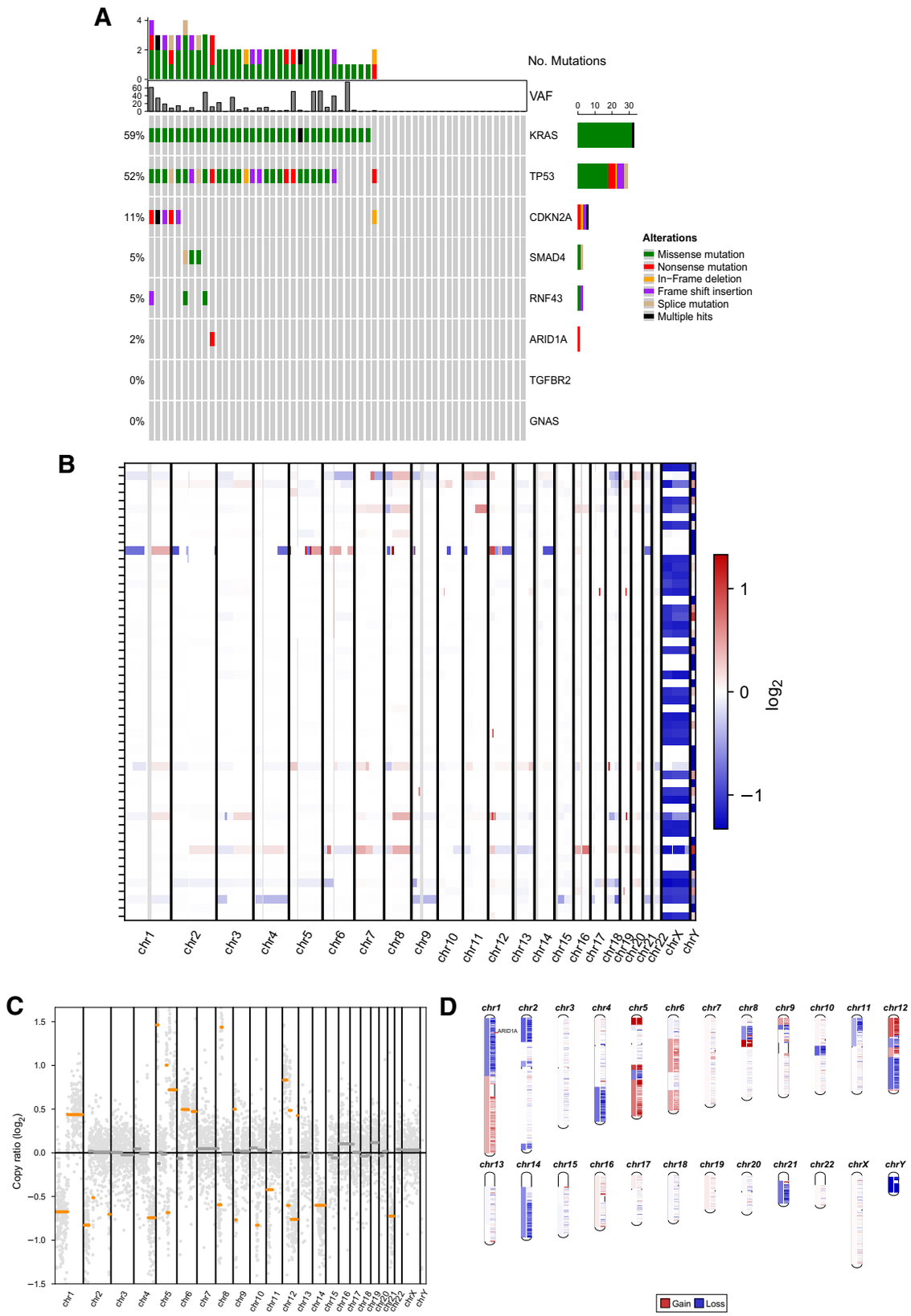

cfDNA and mononuclear cells as input, respectively. The mutation analysis was performed blinded to mutation frequencies and included appropriate control samples.

Statistical analysis

All statistical analyses were performed in IBM SPSS (version 26.0, https://www.ibm.com/products/spss-statistics). All tests were two-sided, and P values <0.05 were considered significant. Clinicopathological patient data were compared using the χ^2 or Fisher's exact test for categorical data, and the independent samples t test or Mann–Whitney U test for continuous data. The Wilcoxon signed-rank test was used to compare matched samples. Survival analyses were performed with Kaplan–Meier estimates, the log-rank test, and Cox proportional hazards regression. Progression-free survival (PFS) was defined as the time between inclusion and progression according to the RECIST criteria, or death due to any cause when the patient died before evidence of progression was obtained. OS was defined as the time between inclusion and death due to any cause. For survival analyses during treatment (samples obtained 1 and 2 months after inclusion), the time elapsed between inclusion and sampling was not included to prevent immortal time bias. Univariable Cox regression analyses were used to investigate the effects of single variables on survival. Multivariable Cox regression modeling was also performed for select variables (i.e., ctDNA point mutation status, CNA status, CA19–9 level, tumor location, clinical stage, ECOG, and first-line treatment). Because of correlation, ctDNA mutation status and CNA status were run in separate models in the multivariable regression. The multivariable analyses were performed with both forward and backward stepwise selection of covariates.

Data availability

The data that support the findings of this study are available from the corresponding authors upon reasonable request. The TagXtractor, SSCScreator, and HYTEC-pipeline.sh scripts are available for download at GitHub (https://github.com/). The PlasmaMutationDetector2 R package is available at CRAN (https://cran.r-project.org/).

Results

ctDNA detection in patients with advanced pancreatic cancer

We measured ctDNA in 56 patients with locally advanced ($n = 8$; 16%) or metastatic ($n = 48$; 84%) pancreatic cancer. The median follow-up time was 6.1 months (range, 0.3–25.8 months). The median age of the cohort was 67 years (range, 41–81 years), and there was a slight majority of men ($n = 35$; 62%). Most patients received either gemcitabine plus nab-paclitaxel ($n = 32$, 57%) or FOLFIRINOX ($n = 17$, 30%). When comparing patients stratified by ctDNA status, as defined by the detection of somatic point mutations or CNA, we found a significant difference between ctDNA-positive and ctDNA-negative patients in regard to sex ($P = 0.025$), median cfDNA level ($P = 1.3E{-}04$), median mode cfDNA fragment size ($P = 3.3E{-}04$), primary tumor location ($P = 0.011$), and M-stage ($P = 0.042$). All baseline patient characteristics and clinicopathological data are summarized in **Table 1**.

The cfDNA samples (input 1–76 ng) were sequenced to a median depth of 66,457 (range, 3,501–158,527; median depth: 2,402 x/ng input). After construction of UMI families, the median number of unique recovered cfDNA templates was 3,584 (range, 154–8,840; median recovery, 22.3%). We performed ddPCR analysis of cfDNA to validate variants and analyzed leukocyte DNA to filter potential CHIP variants (12 variants in 11 patients; Supplementary Table S1). After validation, somatic point mutations were retained in 34/56 (61%; median 2 point mutations) samples obtained at baseline and in 90/268 (33.6%) samples obtained during treatment. Point mutations detected at baseline (**Fig. 1A**; Supplementary Table S2) had a median variant allele frequency (VAF) of 7.7% and occurred most frequently in *KRAS* ($n = 33$), followed by mutations in *TP53* ($n = 29$) and *CDKN2A* ($n = 6$). The majority of patients with detectable *KRAS* mutations at baseline had either G12D ($n = 18$) or G12V ($n = 10$) variants; one patient had dual G12D/G12V variants. Three patients had the G12R variant, and two patients had mutations in either G12C or Q61K. In addition, one patient had a rare activating variant in codon 22 (Q22K; ref. 31). This variant was previously reported in benign intraductal neoplasms of the pancreas (32), but has not previously been reported in pancreatic cancer.

A global z-score ≥4, corresponding to approximately 5% tumor-derived fraction (Supplementary Fig. S1), was used as a cutoff value to classify a cfDNA sample as ctDNA-positive based on CNAs. With this cutoff value, CNAs were detected in 19/55 (34.5%) samples obtained at baseline [one sample failed quality control (QC)], including one sample without detectable point mutations. In samples obtained during treatment, CNAs were detected in 30/243 (12.3%) samples (25 samples failed QC). On the chromosome level, copy-number changes occurred genome-wide, with gains/amplifications in chr12p (including *KRAS*), chr8q (including *MYC*), and chr20q (including *GNAS*) and loss in chr3p (including *TGFBR2*) being the most frequent (**Fig. 1B**). Of the 14 patients with gains/amplifications in chr12p at baseline, all but one had concurrent somatic mutations in *KRAS*. In the last patient sample with chr12p amplification, no point mutations were detected. Instead, this patient had widespread CNAs (**Fig. 1C** and **D**). Notably, only one patient had detectable deletions in chr17p despite *TP53* aberrations being frequently involved in pancreatic cancer.

Prognostic value of ctDNA detection

To determine whether detection of ctDNA at baseline is associated with outcome, we divided patients into groups based on the detection of point mutations (negative vs. positive) and detection of CNAs (negative, z-score < 4 vs. positive, z-score ≥ 4). We found a significant difference in PFS between patients who were point mutation negative and patients who were point mutation positive [6.9 months; 95% confidence interval (CI), 2.8–11 months vs. 2.6 months; 95% CI, 1.4–3.7 months; $P = 2.4E{-}04$; **Fig. 2A**). Similarly, there was a significant difference between CNA-negative patients and CNA-positive patients

Figure 1.

Point mutations and genome-wide copy-number changes detected in cfDNA at baseline. **A,** Oncoprint of point mutations detected in cfDNA. Each row represents a single patient ($n = 56$). Columns represent mutation frequency (left) or mutated gene (right). Bar plots represent number of patients with the mutated gene (right), number of mutations detected in each patient (top), and the highest detected variant allele frequency (VAF) in each patient (second from top). **B,** Copy-number aberrations (CNA) detected across all chromosomes (x-axis) for all patients (y-axis) at baseline ($n = 56$). Copy-number loss is indicated in blue and copy-number gains in red. The gray area indicates excluded regions. **C,** Scatter plot depicting normalized $\log_2$ read-depth values for the baseline sample from a patient with widespread CNAs. Orange bars indicate areas with significant copy-number changes. **D,** Chromosome diagram of copy-number changes in the same patient sample as in **C**. Copy-number loss is indicated in blue and copy-number gains in red.

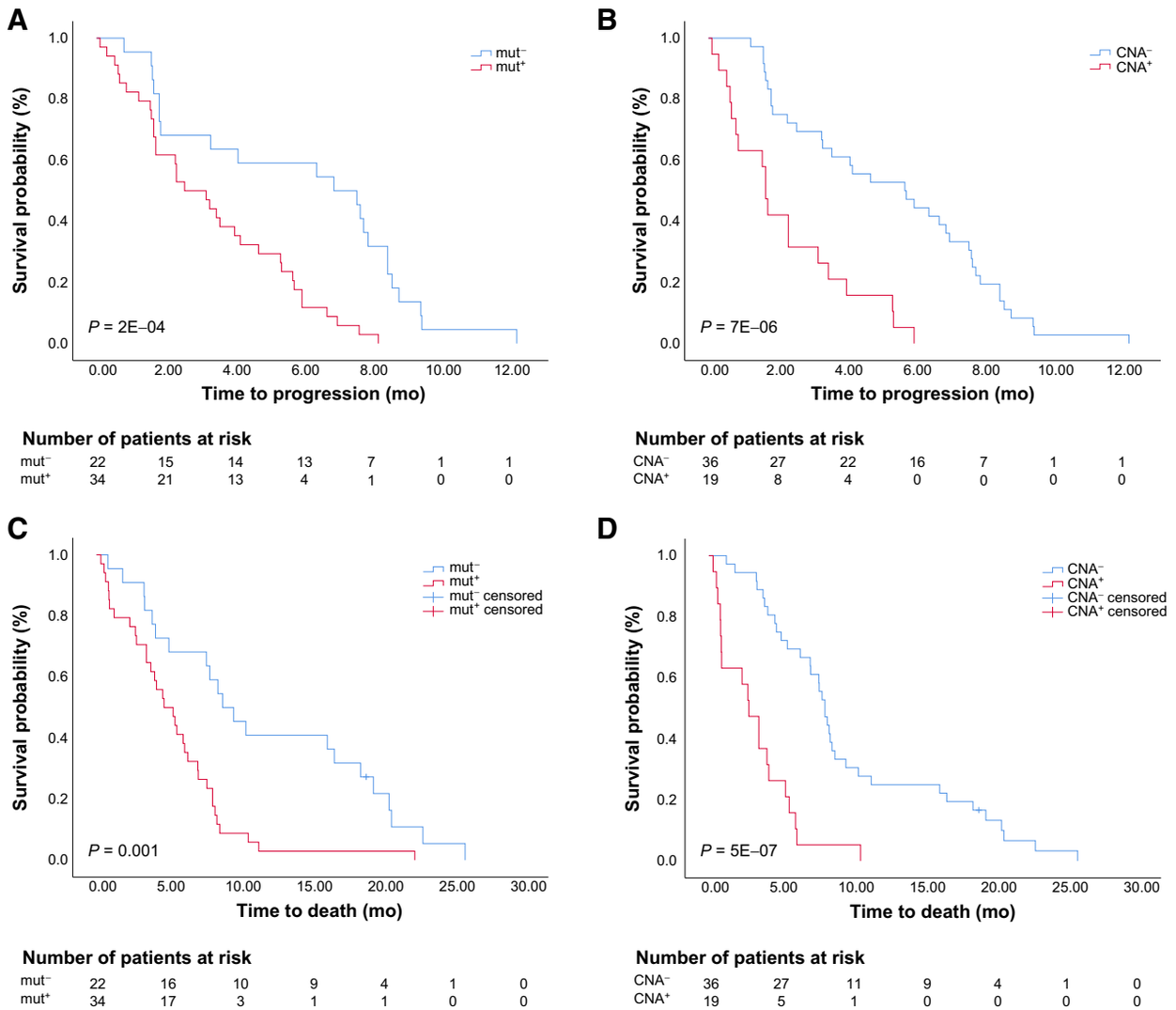

Figure 2.

Kaplan–Meier survival curves according to baseline ctDNA detection. **A** and **B,** Progression-free survival according to baseline ctDNA status based on (**A**) point mutations (mut$^+$ vs. mut$^-$) and (**B**) detectable copy-number aberrations (CNA$^+$ vs. CNA$^-$). **C** and **D,** Overall survival according to baseline ctDNA status based on (**C**) point mutations (mut$^+$ vs. mut$^-$) and (**D**) detectable CNAs (CNA$^+$ vs. CNA$^-$).

(5.7 months; 95% CI, 3.1–8.4 months vs. 1.7 months; 95% CI, 1.4–1.9 months; P = 7E−06; **Fig. 2B**). We also found a significant difference in OS between patients who were point mutation negative and patients who were point mutation positive (8.8 months; 95% CI, 5.9–11.7 months vs. 4.7 months; 95% CI, 2.9–6.6 months; P = 0.001; **Fig. 2C**), and between CNA-negative patients and CNA-positive patients (8.1 months; 95% CI, 7.3–9 months vs. 2.8 months; 95% CI, 1.6–4 months; P = 5.2E−07; **Fig. 2D**).

Univariable and multivariable Cox regression analyses were performed to estimate the prognostic impact of ctDNA point mutation and CNA status relative to other clinicopathological parameters. The univariable regression analyses (Supplementary Table S3) confirmed the prognostic impact of ctDNA detection, as well as that of cfDNA concentration, mode cfDNA size, tumor location, ECOG performance status, and first-line treatment. Multivariable Cox regression analyses were performed in two separate models, as ctDNA point mutation status and CNA status were highly correlated (**Table 2**). These models demonstrated that the dichotomized ctDNA point mutation status (Model A) and CNA status (Model B) were independent prognostic factors for both PFS [hazard ratio (HR), 2.847; P = 0.003; HR, 3.539; P = 3E−04, respectively] and OS (HR, 2.600; P = 0.004; HR, 3.862; P = 6.6E−05, respectively). In addition, ECOG performance status and first-line treatment were independent prognostic factors for both PFS and OS in both models.

Dynamic changes in ctDNA during treatment

Of the 56 patients included in this study, 35 had plasma samples taken at the time of progression. To investigate the dynamic changes in ctDNA, including the impact of chemotherapy, we compared samples obtained before initiation of chemotherapy (baseline) and at the time

Table 2. Multivariable Cox regression.

Model A	Parameter	Progression-free survival		Overall survival	
		Hazard ratio (95% CI)	*P*	Hazard ratio (95% CI)	*P*
	ctDNA point mutation status (mut^+ vs. mut^-)	2.847 (1.427–5.681)	**0.003**	2.600 (1.367–4.946)	**0.004**
	ECOG performance status		**0.024**		**0.006**
	0	Reference		Reference	
	1	1.039 (0.412–2.619)	0.936	0.871 (0.354–2.146)	0.765
	2	2.918 (0.963–8.840)	0.058	3.135 (1.060–9.270)	**0.039**
	First-line treatment		**0.009**		**0.010**
	Gemcitabine	Reference		Reference	
	FOLFIRINOX	0.208 (0.075–0.574)	**0.002**	0.203 (0.072–0.574)	**0.003**
	Gemcitabine + nab-paclitaxel	0.255 (0.095–0.689)	**0.007**	0.293 (0.113–0.761)	**0.012**

Model B	Parameter	Progression-free survival		Overall Survival	
		Hazard Ratio (95% CI)	*P*	Hazard Ratio (95% CI)	*P*
	CNA status (CNA^+ vs. CNA^-)	3.539 (1.785–7.018)	**3E−04**	3.862 (1.988–7.500)	**6.6E−05**
	ECOG performance status		**0.018**		**0.005**
	0	Reference		Reference	
	1	1.123 (0.447–2.817)	0.805	1.146 (0.475–2.762)	0.762
	2	3.374 (1.059–10.747)	**0.040**	4.166 (1.341–12.935)	**0.014**
	First-line treatment		**0.005**		**0.023**
	Gemcitabine	Reference		Reference	
	FOLFIRINOX	0.223 (0.078–0.637)	**0.005**	0.239 (0.084–0.683)	**0.008**
	Gemcitabine + nab-paclitaxel	0.260 (0.099–0.678)	**0.006**	0.322 (0.128–0.811)	**0.016**

of progression, after 1 (B2) and 2 (B3) months of therapy (**Fig. 3A**). Thirty-two patients had samples for all time points. All analyses were based on point mutation detection, as CNA analyses were not sensitive enough to detect small changes in ctDNA levels. A significant decrease in ctDNA VAF was observed after 1 month of therapy ($P = 2E{-}04$) and a further decrease after 2 months of therapy ($P = 0.060$). Paired analysis of samples obtained after 2 months of therapy and at the time of progression also demonstrated a significant increase in ctDNA VAF at the time of progression ($P = 0.003$), after the initial effect of chemotherapy. In contrast, no increase in ctDNA VAF was observed at the time of progression compared with baseline ($P = 0.434$).

As there was an observed effect of chemotherapy on the detection of ctDNA, we hypothesized that ctDNA persistence (i.e., <10-fold reduction in VAF) after initiation of chemotherapy was associated with clinical outcome. To test this hypothesis, we investigated whether there was a difference in PFS between patients with and without ctDNA persistence. After 1 month of therapy, we did not observe any difference in PFS between the groups ($P = 0.822$; **Fig. 3B**). However, patients with ctDNA persistence after 2 months of therapy had a significantly shorter median PFS compared with patients without (0 months; 95% CI, 0–0 months vs. 3.4 months; 95% CI, 1.7–5.1 months; $P = 0.002$; **Fig. 3C**). Four of the six patients with ctDNA persistence after 2 months of therapy had radiologically confirmed progression at the time of sampling. The remaining two patients progressed after 5 or 72 days. In contrast with PFS, shorter median OS was observed for patients with ctDNA persistence after both 1 (3.3 months; 95% CI, 0.1–6.5 months vs. 6.9 months; 95% CI, 5–8.8 months; $P = 0.016$; **Fig. 3D**) and 2 months of therapy (1 month; 95% CI, 0.2–1.8 months vs. 4.2 months; 95% CI, 2.4–6 months; $P = 0.025$; **Fig. 3E**).

Tracking somatic variants to detect disease progression

To evaluate whether mutated ctDNA could be used for monitoring the treatment response and to reveal disease progression earlier than radiological imaging, we examined ctDNA from follow-up blood samples obtained from 27 patients in our cohort. We selected patients with at least two blood draws and one radiological examination after initiation of treatment, and excluded patients lacking follow-up samples at the time of progression and patients who did not provide any positive ctDNA samples. As we did not sequence the primary tumor, we could not establish whether the latter group were low-shedders or had mutations not covered by our sequencing panel. Only point mutations were used to detect ctDNA during follow-up, as CNA analyses were not sensitive enough to detect ctDNA changes.

Radiologically confirmed progression was observed in 25/27 (93%) patients, with a median time to progression of 126 days. Two patients died because of pancreatic cancer without radiologically confirmed progression at 152 days of follow-up. A >25% increase in ctDNA was observed for 17/27 (63%) patients, including the two patients who died without confirmed progression (**Fig. 4A**). Interestingly, both of these patients succumbed within 1 month of the detected increase in ctDNA. By including ctDNA persistence, the number of patients in whom ctDNA detected progression increased to 19/27 (70%) patients. Similarly, using a threshold of >50% increase in CA19–9 during therapy, CA19–9 also detected progression in 17/27 (63%) patients with radiologically confirmed progression or who died without confirmed progression. In many cases, ctDNA and CA19–9 exhibited similar dynamic patterns (**Fig. 4B**). However, we also observed cases in which ctDNA and CA19–9 levels presented conflicting results (**Fig. 4C** and **D**). In one patient, ctDNA increased 84 days before progression, but also 63 days before an increase in CA19–9 levels was observed (**Fig. 4C**). In another patient, ctDNA levels increased at the time of progression after an initial drop after therapy initiation, whereas CA19–9 levels dropped at the time of progression after an initial increase (**Fig. 4D**). When we assessed the time between the increase in ctDNA VAF and the time of radiologically detected progression/time of death, the median lead time was 22 days ($P = 0.002$; **Fig. 4A**). Similarly, the median lead time of the combined ctDNA increase/

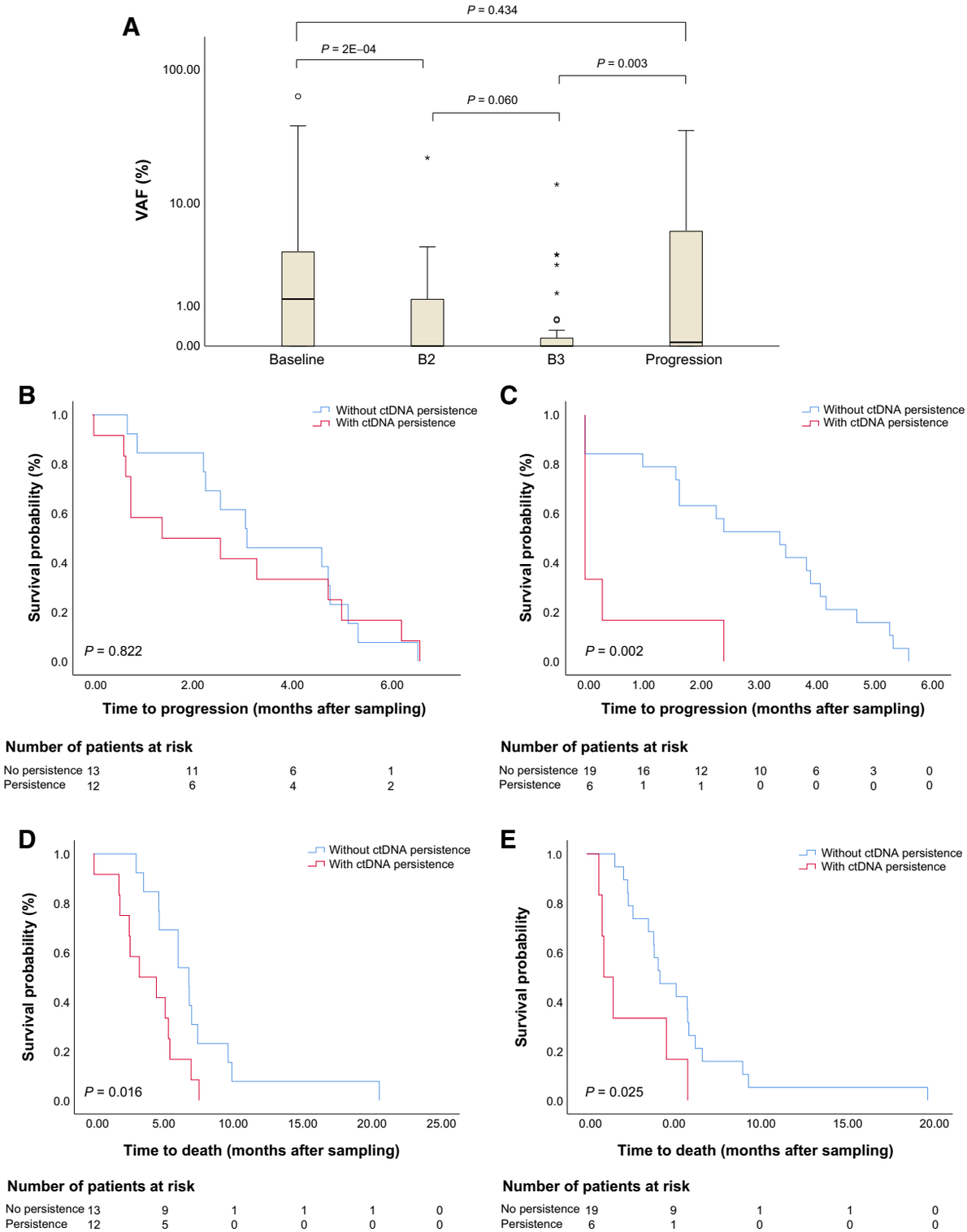

Figure 3.

Dynamic changes in ctDNA during treatment. **A,** Boxplot of ctDNA VAF at baseline, 1 (B2) and 2 months (B3) after initiation of chemotherapy, and at the time of progression ($n = 32$). **B,** Progression-free survival in patients without ctDNA persistence versus patients with ctDNA persistence 1 month after initiation of chemotherapy and (**C**) 2 months after initiation of chemotherapy. **D,** Overall survival in patients without ctDNA persistence versus patients with ctDNA persistence 1 month after initiation of chemotherapy and (**E**) 2 months after initiation of chemotherapy.

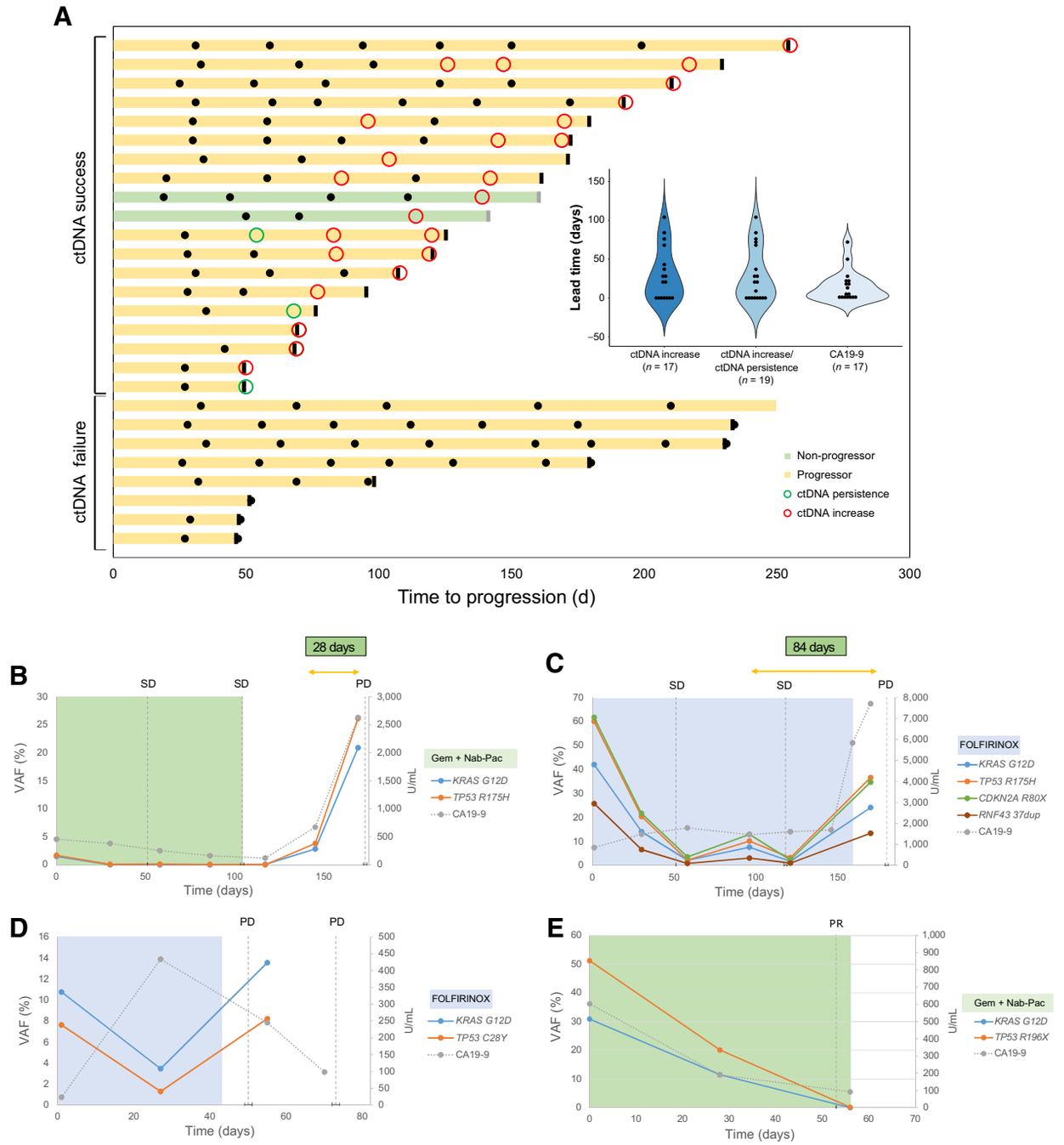

Figure 4.

Longitudinal monitoring of disease progression by ctDNA. **A,** ctDNA surveillance in 27 patients demonstrated the ability of mutant ctDNA (red and green circles) to detect progression and death. Patients were censored at the time of radiologically detected progression (black bar) or death (gray bar). Inset image depicts lead time in detecting progression/death by ctDNA and CA19–9 compared with progression by radiological imaging/death due to pancreatic cancer. **B–E,** ctDNA monitoring to detect progression and response in four patients with advanced pancreatic cancer. SD, stable disease; PD, progressive disease; PR, partial response. Color-coding indicates treatment regimen.

ctDNA persistence was 19 days ($P = 0.002$). In comparison, the median lead time using the CA19–9 increase to detect progression/death was 6 days ($P = 0.007$; **Fig. 4A**), which was not significantly shorter than the lead time with either the ctDNA increase alone or ctDNA increase/ctDNA persistence ($P = 0.161$ and $P = 0.123$, respectively). In addition to detecting progression, our results also demonstrated that longitudinal monitoring of ctDNA and CA19–9 levels could be used to detect the response to therapy (**Fig. 4E**).

Discussion

Several clinical applications have been proposed for ctDNA, including early detection of disease, prediction of clinical outcome, monitoring of treatment response, detection of residual disease and relapse in early stages, detection of progression and emergence of resistance mutations in advanced cancers, and as a biomarker to guide treatment selection (33, 34). In this study, we investigated the prognostic value of ctDNA, the ctDNA dynamics, and the monitoring potential of ctDNA in patients with advanced pancreatic cancer.

We demonstrated that ctDNA persistence, that is, the lack of ctDNA clearance, shortly after chemotherapy initiation is associated with shorter PFS and OS (**Fig. 3**). Groot and colleagues (35) presented similar results for patients with operable pancreatic cancer, as persistence or emergence of ctDNA in the immediate postoperative period was associated with shorter recurrence-free survival. In accordance with our results, Yu and colleagues (36) also demonstrated that ctDNA persistence is prognostic for advanced cancer. In their study, persistent *EGFR*-mutant ctDNA after 6 weeks of treatment in patients with metastatic *EGFR*-mutant lung cancer was associated with shorter PFS and OS. Our findings should be interpreted carefully, as very few patients were included in the analysis. Nonetheless, we suggest that ctDNA persistence could be used to identify patients with a lack of response to treatment.

The current evidence for the potential utility of longitudinal monitoring of ctDNA in patients with pancreatic cancer is mostly limited to small studies with few patients (16, 18–20, 35, 37–39). Perhaps the strongest evidence is provided by Groot and colleagues (35), who demonstrated that ctDNA detected disease recurrence in 27/30 (90%) patients with localized pancreatic cancer, with a median lead time of 84 days relative to radiological imaging. In patients with advanced pancreatic cancer, Bernard and colleagues (38) demonstrated a median lead time of 50 days relative to imaging, significantly better than using CA19–9 for monitoring. However, in this case, the detection of disease progression was based on DNA derived from extracellular vesicles, whereas mutated ctDNA were not associated with outcome. In contrast, Kruger and colleagues (19) demonstrated that *KRAS*-mutated ctDNA could detect disease progression in 20/24 (83%) patients with advanced pancreatic cancer. They also demonstrated that ctDNA detects progression earlier than imaging, though it was not significantly better than that of CA19–9. Recently, Guan and colleagues (39) demonstrated a lead time of 27 days in the detection of progression using ctDNA compared with radiological imaging in a cohort of 24 patients with advanced pancreatic cancer. In the current study, disease progression was detected by ctDNA in 19/27 (70%) patients with radiologically confirmed progression or who died from pancreatic cancer without confirmed progression (**Fig. 4**). The median lead time for progression detected by ctDNA was 19 days, compared with 6 days for CA19–9, which is comparable with previous studies (19, 39).

Discrepancies between disease progressions detected by ctDNA and radiologically confirmed progression were observed for several of the monitored patients in this study. Although we are likely missing low VAF mutations due to biological/technical issues, we should not exclude the possibility that radiologically determined responses could be erroneous. The major disadvantage of RECIST is that it relies on subjective image interpretation (40). Consequently, both intra- and interobserver variability occur in response evaluation, with the largest variation observed when measuring multiple targets (41, 42). Furthermore, pancreatic cancer is known for abundant fibrosis, which could be induced by treatment (43) and further complicate the evaluation of responses for this tumor type. Nevertheless, nearly every observed increase in ctDNA was followed by radiologically confirmed progression. The exception was two cases with evidence of progression despite it not being detected by radiological imaging. The first patient had a tumor that was difficult to measure for the radiologist at the point when ctDNA levels increased, which exemplifies the uncertainties of using the RECIST criteria. The other patient had their last CT scan almost 2 months before the detected increase in ctDNA. Both patients died within a month of the ctDNA increase, suggesting progressive disease. Our findings are comparable with the results reported by Kruger and colleagues (19), who demonstrated 100% specificity of ctDNA in detecting disease progression, indicating that ctDNA may be a promising monitoring biomarker in patients with advanced pancreatic cancer despite apparent limitations in sensitivity. In contrast with increases in ctDNA, spikes in CA19–9 levels were observed in three patients with no association with progression, and levels returned to baseline in the next follow-up sample.

An issue in ctDNA detection in pancreatic cancer is that these tumors are known for shedding low levels of cfDNA compared with other cancers (44, 45). Thus, even patients with advanced disease may have low levels of ctDNA. Although our sequencing method is capable of detecting mutations down to 0.1% VAF (23), it likely misses ctDNA due to methodological and biological limitations. Our results demonstrate that cfDNA levels are significantly lower in ctDNA-negative samples than in ctDNA-positive samples (**Table 1**), indicating that increasing the amount of plasma for cfDNA isolation is important for detecting ctDNA in patients with low shedding of cfDNA into the circulation. The majority of our patient samples contained less than 50-ng cfDNA, which would be required to call rare mutations (down to 0.1% VAF) with confidence. To overcome sensitivity issues, different methods for detecting ctDNA have been proposed, including cfDNA fragment analysis (46, 47) and DNA methylation (48, 49), which have both shown an improved ability to detect ctDNA compared with mutation detection. We are currently exploring these options in a separate study.

The additional analysis of CNA only added a single ctDNA-positive patient apart from the patients identified using somatic mutation analysis. Because of the low sensitivity of the analysis (corresponding to ∼5% VAF), the CNA-positive patients constitute a high-VAF ctDNA group. However, CNA analysis provided additional insights into tumor development. For example, almost all patients with gains/amplifications in chr12p also had somatic mutations in *KRAS*. We were also able to detect gains/amplifications in chr20q (containing *GNAS*) in multiple patients, though we did not detect any somatic mutations in *GNAS*.

Our study has several limitations. First, we did not have access to tumor tissue as core/fine needle biopsies are not part of standard clinical care. Thus, it is possible that some patients had point mutations in genes not covered by our sequencing panel. Using a tumor-informed approach would also have enabled us to use a less stringent method to call mutations, which could have allowed ctDNA detection in additional patient samples. Second, because of the generally poor condition of our patients, we had difficulties maintaining regular serial blood sample collection in some patients. Third, the number of patients included, especially in the ctDNA dynamics and monitoring part of the study, was rather low. Finally, we isolated cfDNA from an equivalent of <2 mL of plasma. Increasing the amount of plasma used would likely have improved the detection of ctDNA.

Conclusions

We confirmed the prognostic value of ctDNA and provided evidence that ctDNA can be used for disease monitoring in advanced

pancreatic cancer. Our results show that ctDNA levels decrease upon the initiation of chemotherapy and subsequently increase at the time of progression. Furthermore, our results suggest that ctDNA persistence is a marker of treatment failure and that longitudinal monitoring of ctDNA can detect disease progression, despite limitations in sensitivity. Although ctDNA is not detected in all patients during the course of the disease, increases in ctDNA that are detected during longitudinal monitoring are highly specific to disease progression. Nevertheless, future prospective and interventional clinical trials of sequential measurements of ctDNA will be required to determine whether ctDNA dynamics can be used to guide treatment selection or changes and whether this can improve outcomes for patients with pancreatic cancer.

Authors' Disclosures

M. Lapin reports grants from Western Norway Regional Health Authorities and The Folke Hermansen Foundation during the conduct of the study. K.H. Edland reports grants from Folke Hermansen Foundation during the conduct of the study. O. Nordgård reports grants from The Western Norway Health Authorities, Folke Hermansen foundation, and The Norwegian Cancer Society during the conduct of the study. No disclosures were reported by the other authors.

Disclaimer

The funding bodies had no role in the design of the study; in the collection, analysis, and interpretation of data; or in the writing of the article.

Authors' Contributions

M. Lapin: Conceptualization, formal analysis, supervision, funding acquisition, investigation, visualization, writing–original draft; writing–review and editing. **K.H. Edland:** Resources, investigation, writing–review and editing. **K. Tjensvoll:** Conceptualization, formal analysis, investigation, writing–review and editing. **S. Oltedal:** Investigation, writing–review and editing. **M. Austdal:** Formal analysis, investigation, visualization, writing–review and editing. **H. Garresori:** Resources, investigation, writing–review and editing. **Y. Rozenholc:** Software, formal analysis, writing–review and editing. **B. Gilje:** Conceptualization, resources, formal analysis, supervision, funding acquisition, project administration, writing–review and editing. **O. Nordgård:** Conceptualization, resources, software, formal analysis, supervision, funding acquisition, investigation, visualization, project administration, writing–review and editing.

Acknowledgments

The authors would like to express our deepest gratitude to the participating patients and their families. We would also like to acknowledge our user/next-of-kin participants Thor Viggo Aarrestad and Eirik Salvesen for their constructive criticism along the way, and radiologist Ole Jacob Greve for assistance on issues regarding radiology. The Folke Hermansen Foundation, the Norwegian Cancer Society (National Group of Expertise for Research on pancreatic cancer), and the Western Norway Regional Health Authorities supported this project financially. The project was part of a strategic program called, "Personalized medicine-biomarkers and clinical studies," supported by the Western Norway Regional Health Authority.

The publication costs of this article were defrayed in part by the payment of publication fees. Therefore, and solely to indicate this fact, this article is hereby marked "advertisement" in accordance with 18 USC section 1734.

Note

Supplementary data for this article are available at Clinical Cancer Research Online (http://clincancerres.aacrjournals.org/).

Received November 15, 2022; revised January 12, 2023; accepted January 18, 2023; published first January 20, 2023.

References

1. Ferlay J, Colombet M, Soerjomataram I, Dyba T, Randi G, Bettio M, et al. Cancer incidence and mortality patterns in Europe: estimates for 40 countries and 25 major cancers in 2018. Eur J Cancer 2018;103:356–87.
2. Carioli G, Bertuccio P, Boffetta P, Levi F, La Vecchia C, Negri E, et al. European cancer mortality predictions for the year 2020 with a focus on prostate cancer. Ann Oncol 2020;31:650–8.
3. Siegel RL, Miller KD, Jemal A. Cancer statistics, 2020. CA Cancer J Clin 2020;70:7–30.
4. Conroy T, Desseigne F, Ychou M, Bouché O, Guimbaud R, Bécouarn Y, et al. FOLFIRINOX versus gemcitabine for metastatic pancreatic cancer. N Engl J Med 2011;364:1817–25.
5. Von Hoff DD, Ervin T, Arena FP, Chiorean EG, Infante J, Moore M, et al. Increased survival in pancreatic cancer with nab-paclitaxel plus gemcitabine. N Engl J Med 2013;369:1691–703.
6. Goldstein D, El-Maraghi RH, Hammel P, Heinemann V, Kunzmann V, Sastre J, et al. nab-Paclitaxel plus gemcitabine for metastatic pancreatic cancer: long-term survival from a phase III trial. J Natl Cancer Inst 2015;107:dju413.
7. Hidalgo M. Pancreatic cancer. N Engl J Med 2010;362:1605–17.
8. Tempero MA, Uchida E, Takasaki H, Burnett DA, Steplewski Z, Pour PM. Relationship of carbohydrate antigen 19–9 and Lewis antigens in pancreatic cancer. Cancer Res 1987;47:5501–3.
9. Marrelli D, Caruso S, Pedrazzani C, Neri A, Fernandes E, Marini M, et al. CA19–9 serum levels in obstructive jaundice: clinical value in benign and malignant conditions. Am J Surg 2009;198:333–9.
10. Ballehaninna UK, Chamberlain RS. The clinical utility of serum CA 19–9 in the diagnosis, prognosis and management of pancreatic adenocarcinoma: an evidence-based appraisal. J Gastrointest Oncol 2012;3:105–19.
11. Dawson SJ, Tsui DW, Murtaza M, Biggs H, Rueda OM, Chin SF, et al. Analysis of circulating tumor DNA to monitor metastatic breast cancer. N Engl J Med 2013;368:1199–209.
12. Vidal J, Muinelo L, Dalmases A, Jones F, Edelstein D, Iglesias M, et al. Plasma ctDNA RAS mutation analysis for the diagnosis and treatment monitoring of metastatic colorectal cancer patients. Ann Oncol 2017;28:1325–32.
13. Christensen E, Birkenkamp-Demtröder K, Sethi H, Shchegrova S, Salari R, Nordentoft I, et al. Early detection of metastatic relapse and monitoring of therapeutic efficacy by ultra-deep sequencing of plasma cell-free DNA in patients with urothelial bladder carcinoma. J Clin Oncol 2019;37:1547–57.
14. Wan JCM, Heider K, Gale D, Murphy S, Fisher E, Mouliere F, et al. ctDNA monitoring using patient-specific sequencing and integration of variant reads. Sci Transl Med 2020;12:eaaz8084.
15. Lapin M, Oltedal S, Tjensvoll K, Buhl T, Smaaland R, Garresori H, et al. Fragment size and level of cell-free DNA provide prognostic information in patients with advanced pancreatic cancer. J Transl Med 2018;16:300.
16. Tjensvoll K, Lapin M, Buhl T, Oltedal S, Steen-Ottosen Berry K, Gilje B, et al. Clinical relevance of circulating KRAS mutated DNA in plasma from patients with advanced pancreatic cancer. Molecular Oncology 2016;10:635–43.
17. Zill OA, Greene C, Sebisanovic D, Siew LM, Leng J, Vu M, et al. Cell-free DNA next-generation sequencing in pancreatobiliary carcinomas. Cancer Discov 2015;5:1040–8.
18. Cheng H, Liu C, Jiang J, Luo G, Lu Y, Jin K, et al. Analysis of ctDNA to predict prognosis and monitor treatment responses in metastatic pancreatic cancer patients. Int J Cancer 2017;140:2344–50.
19. Kruger S, Heinemann V, Ross C, Diehl F, Nagel D, Ormanns S, et al. Repeated mutKRAS ctDNA measurements represent a novel and promising tool for early response prediction and therapy monitoring in advanced pancreatic cancer. Ann Oncol 2018;29:2348–55.
20. Perets R, Greenberg O, Shentzer T, Semenisty V, Epelbaum R, Bick T, et al. Mutant KRAS circulating tumor DNA is an accurate tool for pancreatic cancer monitoring. Oncologist 2018;23:566–72.
21. Wei T, Zhang Q, Li X, Su W, Li G, Ma T, et al. Monitoring tumor burden in response to FOLFIRINOX chemotherapy via profiling circulating cell-free DNA in pancreatic cancer. Mol Cancer Ther 2019;18:196–203.
22. Witkiewicz AK, McMillan EA, Balaji U, Baek G, Lin WC, Mansour J, et al. Whole-exome sequencing of pancreatic cancer defines genetic diversity and therapeutic targets. Nat Commun 2015;6:6744.

23. Tjensvoll K, Lapin M, Gilje B, Garresori H, Oltedal S, Forthun RB, et al. Novel hybridization- and tag-based error-corrected method for sensitive ctDNA mutation detection using ion semiconductor sequencing. Sci Rep 2022;12:5816.
24. Eisenhauer EA, Therasse P, Bogaerts J, Schwartz LH, Sargent D, Ford R, et al. New response evaluation criteria in solid tumours: revised RECIST guideline (version 1.1). Eur J Cancer 2009;45:228–47.
25. Li H, Handsaker B, Wysoker A, Fennell T, Ruan J, Homer N, et al. The sequence alignment/map format and SAMtools. Bioinformatics 2009;25:2078–9.
26. Li H, Durbin R. Fast and accurate long-read alignment with Burrows–wheeler transform. Bioinformatics 2010;26:589–95.
27. Pécuchet N, Rozenholc Y, Zonta E, Pietrasz D, Didelot A, Combe P, et al. Analysis of base-position error rate of next-generation sequencing to detect tumor mutations in circulating DNA. Clin Chem 2016;62:1492–503.
28. Koboldt DC, Zhang Q, Larson DE, Shen D, McLellan MD, Lin L, et al. VarScan 2: somatic mutation and copy-number alteration discovery in cancer by exome sequencing. Genome Res 2012;22:568–76.
29. Talevich E, Shain AH, Botton T, Bastian BC. CNVkit: genome-wide copy number detection and visualization from targeted DNA sequencing. PLoS Comput Biol 2016;12:e1004873.
30. Amemiya HM, Kundaje A, Boyle AP. The ENCODE blacklist: identification of problematic regions of the genome. Sci Rep 2019;9:9354.
31. Tsukuda K, Tanino M, Soga H, Shimizu N, Shimizu K. A novel activating mutation of the K-ras gene in human primary colon adenocarcinoma. Biochem Biophys Res Commun 2000;278:653–8.
32. Amato E, Molin MD, Mafficini A, Yu J, Malleo G, Rusev B, et al. Targeted next-generation sequencing of cancer genes dissects the molecular profiles of intraductal papillary neoplasms of the pancreas. J Pathol 2014;233:217–27.
33. Pascual J, Attard G, Bidard FC, Curigliano G, De Mattos-Arruda L, Diehn M, et al. ESMO recommendations on the use of circulating tumour DNA assays for patients with cancer: a report from the ESMO Precision Medicine Working Group. Ann Oncol 2022;33:750–68.
34. Nordgård O, Brendsdal Forthun R, Lapin M, Grønberg BH, Kalland KH, Kopperud RK, et al. Liquid biopsies in solid cancers: implementation in a nordic healthcare system. Cancers 2021;13:1861.
35. Groot VP, Mosier S, Javed AA, Teinor JA, Gemenetzis G, Ding D, et al. Circulating tumor DNA as a clinical test in resected pancreatic cancer. Clin Cancer Res 2019;25:4973–84.
36. Yu HA, Schoenfeld AJ, Makhnin A, Kim R, Rizvi H, Tsui D, et al. Effect of osimertinib and bevacizumab on progression-free survival for patients with metastatic EGFR-mutant lung cancers: a phase 1/2 single-group open-label trial. JAMA Oncol 2020;6:1048–54.
37. Sausen M, Phallen J, Adleff V, Jones S, Leary RJ, Barrett MT, et al. Clinical implications of genomic alterations in the tumour and circulation of pancreatic cancer patients. Nat Commun 2015;6:7686.
38. Bernard V, Kim DU, San Lucas FA, Castillo J, Allenson K, Mulu FC, et al. Circulating nucleic acids are associated with outcomes of patients with pancreatic cancer. Gastroenterology 2019;156:108–18.
39. Guan S, Deng G, Sun J, Han Q, Lv Y, Xue T, et al. Evaluation of circulating tumor DNA as a prognostic biomarker for metastatic pancreatic adenocarcinoma. Front Oncol 2022;12:926260.
40. Villaruz LC, Socinski MA. The clinical viewpoint: definitions, limitations of RECIST, practical considerations of measurement. Clin Cancer Res 2013;19:2629–36.
41. Suzuki C, Torkzad MR, Jacobsson H, Åström G, Sundin A, Hatschek T, et al. Interobserver and intraobserver variability in the response evaluation of cancer therapy according to RECIST and WHO-criteria. Acta Oncol 2010;49:509–14.
42. Kuhl CK, Alparslan Y, Schmoee J, Sequeira B, Keulers A, Brümmendorf TH, et al. Validity of RECIST Version 1.1 for response assessment in metastatic cancer: a prospective, multireader study. Radiology 2019;290:349–56.
43. Erstad DJ, Sojoodi M, Taylor MS, Jordan VC, Farrar CT, Axtell AL, et al. Fibrotic response to neoadjuvant therapy predicts survival in pancreatic cancer and is measurable with collagen-targeted molecular MRI. Clin Cancer Res 2020;26:5007–18.
44. Bettegowda C, Sausen M, Leary RJ, Kinde I, Wang Y, Agrawal N, et al. Detection of circulating tumor DNA in early- and late-stage human malignancies. Sci Transl Med 2014;6:224ra24.
45. Gerratana L, Movarek M, Wehbe F, Katam N, Mahalingam D, Donahue J, et al. Genomic landscape of advanced solid tumors in circulating tumor DNA and correlation with tissue sequencing: a single institution's experience. JCO Precis Oncol 2022;6:e2100289.
46. Mouliere F, Chandrananda D, Piskorz AM, Moore EK, Morris J, Ahlborn LB, et al. Enhanced detection of circulating tumor DNA by fragment size analysis. Sci Transl Med 2018;10:eaat4921.
47. Cristiano S, Leal A, Phallen J, Fiksel J, Adleff V, Bruhm DC, et al. Genome-wide cell-free DNA fragmentation in patients with cancer. Nature 2019;570:385–9.
48. Liu MC, Oxnard GR, Klein EA, Swanton C, Seiden MV. Sensitive and specific multi-cancer detection and localization using methylation signatures in cell-free DNA. Ann Oncol 2020;31:745–59.
49. Shen SY, Singhania R, Fehringer G, Chakravarthy A, Roehrl MHA, Chadwick D, et al. Sensitive tumour detection and classification using plasma cell-free DNA methylomes. Nature 2018;563:579–83.